Short Communication:

Drug-Molecule Adsorption onto Silicon-Doped Fullerene: A Density Functional Theory Study

Yosephine Novita Apriati, Bambang Kristiawan, Nikmatul Jannah, Ari Dwi Nugraheni, and Sholihun Sholihun*

Computational Physics Research Group, Department of Physics, Faculty of Mathematics and Natural Sciences, Universitas Gadjah Mada, Sekip Utara, Yogyakarta 55281, Indonesia

* ***Corresponding author:***

email: sholihun@ugm.ac.id

Received: May 2, 2023
Accepted: July 3, 2023

DOI: 10.22146/ijc.84174

Abstract: *Density functional theory calculations were performed to study the interactions between the host material Si-doped fullerene and the drug molecules paracetamol, a pain and fever reducer, and hydroxyurea, a drug for leukemic treatment. All atoms were relaxed so that the atomic force was less than 5.0 × 10^{-3} eV/Å. Structural and electronic properties, such as adsorption energy, formation energy, and charge transfer, were calculated. Results showed that Si-doped fullerene had more negative adsorption energy and lower formation energy than undoped fullerene, indicating that drug molecules could be chemisorbed in Si-doped fullerene. These results contribute to the future drug delivery application.*

Keywords: *fullerene; paracetamol; hydroxyurea; adsorption energy; charge transfer*

■ INTRODUCTION

Reducing the inevitable side effects of drugs is currently becoming the main issue in drug development [1-2]. A drug delivery system is one popular method for solving the above problem. Drug delivery with a nanoscale delivery vehicle can minimize the side effects of drugs and enhance the efficacy of the associated drugs [3]. A nanoparticle, such as a fullerene, with a specific geometry, size, surface characteristics, unique structure, and strong polarity [4], can be used as a lipid-like system and even cross-cell membranes [5]. C_{60} is an appropriate structure for drug delivery given that its synthesized composition consists of 60 carbon atoms, 12 pentagons (5–5 single bonds), and 20 hexagons (5–6 double bonds) [6-7]. Previous work investigated C_{60} as a potential drug carrier and showed that fullerene maintains small molecules (H_2O, O_3, H_2, NH_3, and O_2) in a stable state [8-14].

Studies on drug sensors using C_{60} have attracted considerable attention because of the importance of fullerene as a drug abuse detector. These works focused on calculating the adsorption energy of the drug for fullerene. The results showed that drug molecules, such as amphetamine and phenylpropanolamine, can be adsorbed onto fullerene through the introduction of an atom dopant. An atom dopant can increase the conductivity and reactivity of fullerene toward a drug, conferring fullerene with good potential as a drug abuse detector [10-11]. Given that doped C_{60} is a potentially good drug detector, it is also possible to apply doped C_{60} as a drug delivery system with a similar structure.

The application of fullerene as a drug delivery system has been studied in recent years [10-11,15]. Amantadine, a drug for the treatment of Parkinson's disease, was investigated by using density functional theory (DFT). The results showed that pure C_{60} had a weak interaction with the drug and was thus not an adequate amantadine carrier. Doping atoms were used to increase the reactivity of the C_{60} surface, resulting in the increased adsorption of the drug onto doped C_{60} [12]. The cancer drug 5-fluorouracil was adsorbed onto doped C_{60} [13]. DFT calculations showed that 4-phenylpyridine, a drug for the therapy of Alzheimer's disease, was physisorbed onto C_{60} and chemisorbed onto doped C_{60} [15]. The doped C_{60} successfully increased the

reactivity of fullerene because it decreased the bandgap and increased charge transfer and adsorption [16-17].

In the present work, the potential of C_{60} and Si-doped C_{60} as drug delivery systems for hydroxyurea ($CH_4N_2O_2$) and paracetamol ($C_8H_9NO_2$) was analyzed. Hydroxyurea is a cancer drug that is used to treat acute leukemic, and paracetamol is a common drug used to treat fever and pain. The focus of this work is to study the interactions of these drugs with fullerene. The adsorption energy, formation energy, and charge transfer between the drug and fullerene were calculated.

■ COMPUTATIONAL DETAILS

Geometry optimization and energy calculations were carried out by using the DFT code PHASE/0 [18-21]. The generalized gradient approximation was chosen as the exchange–correlation functional [22]. All systems were modeled in a $25 \times 25 \times 25$ Å^3 square box. Here, 30 Ry and an eight-point mesh grid were applied as the cut-off energy for Brillouin zone integration, respectively. During optimization, all atoms were relaxed until the atomic forces reached 5.0×10^{-3} eV/Å. For the analysis of the interaction between fullerene and drug molecules, the adsorption energy was calculated by using Eq. (1).

$$E_{ads} = E_s - \left(E_{fullerene} + E_{drugs}\right) \quad (1)$$

where E_s is the energy of the system, and $E_{fullerene}$ and E_{drugs} are the total energies of the optimized geometries of fullerene and drug molecules, respectively. Negative adsorption energies indicate that interaction is exothermic and geometrically stable [23]. The stability interaction parameter of the Si-doped fullerene and the drug was calculated based on formation energy by using Eq. (2) [24];

$$E_f = E_s - \left(E_{fullerene+drugs} + \mu C + \mu X\right) \quad (2)$$

where $E_{fullerene+drugs}$ is the energy of the system containing pure fullerene with the drug, while μC and μX are the electronic chemical potentials of the doped C and X atoms, respectively (in this case, X = Si atom).

The energy gap E_g is calculated based on the energy difference between the highest occupied molecular orbital (HOMO) and the lowest unoccupied molecular orbital [25-26]. Ligand binding is an important aspect of drug design exploration. Even though several processes may be involved in this process, partial charge transfer occurs through covalent bonding, dative bonding, or hydrogen bonding [27]. The system acquires an additional electronic charge when an interaction occurs between fullerene and drug molecules. A qualitative approach that measured the electrophilic power of a ligand was suggested to understand the reactivity of the HIV-1 nucleocapsid protein p7 with a variety of electrophilic agents [28]. The global electrophilicity index ω was calculated by using Eq. (3-5);

$$\omega = \frac{\mu^2}{2\eta} \quad (3)$$

$$\mu = \frac{E_{HOMO} + E_{LUMO}}{2} \quad (4)$$

$$\eta = \frac{-E_{HOMO} - \left(-E_{LUMO}\right)}{2} \quad (5)$$

where μ and η are the chemical potential and chemical hardness of a system, respectively. The global interaction of fullerene and the drugs is determined by ΔN, which represents the fractional number of electrons transferred from one system to another system [29]. In association with global electrophilicity, the maximum electronic charge ΔN_{max} is defined by using Eq. (6).

$$\Delta N_{max} = \mu\eta \quad (6)$$

The electrophilicity of a system could be written in terms of ΔN_{max} as Eq. (7);

$$\omega = \frac{\mu^2}{2\eta} = \left(\frac{-\mu}{2}\right)\left(\frac{-\mu}{\eta}\right) = \frac{\chi\Delta_{max}}{2} \quad (7)$$

where ω is the electronegativity of the system and X = 1/χ. Therefore, it becomes Eq. (8).

$$\Delta N_{max} = 2\omega/\chi = 2\omega X \quad (8)$$

Then, if two systems A and B, approach each other, the number of charge transfers between systems in terms of electrophilicity is determined by the electrophilicity-based charge transfer (ECT) as written in Eq. (9).

$$ECT = \left(\Delta N_{max}\right)_A - \left(\Delta N_{max}\right)_B = 2\left\{\omega_A X_A - \omega_B X_B\right\} \quad (9)$$

ECT < 0 indicates that charges flow from A to B such that system A acts as the electron donor, whereas ECT > 0 indicates that charges flow from B to A such that system A acts as an electron acceptor [29]. The open-source program VESTA was used to generate the plot of charge difference distribution [30]. The plot was obtained by subtracting the total charge of the adsorption system from the drug system and fullerene or

doped fullerene with the individual charge of an isolated drug and host material [31-32] as Eq. (10).

$$\Delta\rho = \rho_{pristine+drug} - \left(\rho_{pristine} + \rho_{drug}\right) \quad (10)$$

$P_{pristine+drug}$ is the total charge of the system of fullerene or doped fullerene with drug molecules, and $\rho_{pristine}$ and ρ_{drug} are the total charge of individual isolated fullerene or doped fullerene and the drug, respectively.

■ RESULTS AND DISCUSSION

Optimized Geometries

Drug molecules

Fig. 1 shows the optimized geometries and molecular electronic potentials (MEP) of paracetamol and hydroxyurea, respectively. The MEP plot shows a color spectrum from red to blue that represents the attractiveness of the area around the drug molecules in descending order [33]. The MEP plot is determined by the electric potential at a given point around the molecule as a force acting on a positive test charge [34]. The MEP plots of the paracetamol (Fig.1(a)) and hydroxyurea (Fig. 1(b)) molecules show that the attractive area is near the oxygen atom (red MEP plot around the atom), indicating that the specific oxygen atom on each drug molecule is the sufficient site for the creation of a bond when it interacts with other molecules. Previous molecular electrostatic potential mapped molecular van-der Walls surface of HU was reported to have similar local minima at the oxygen atom [35].

Fullerene and Si-doped fullerene with the drug molecules

The optimized geometries of C_{60} and Si-doped C_{60} are presented in Fig. 2. The substitutional Si is 0.7 Å distorted from the fullerene surface. The newly created bond length between Si–C is about 1.89 Å stretched from the corresponding C–C bond in the pristine C_{60}. The increase in the bond length of C–Si causes the hexagonal bond angle around the Si atom to decrease by ~19°. Our result agrees with that of the previous DFT study based on B3LYP functional, e.g., the C–Si bond in the Si-doped C_{70} is distorted out of plane [36]. Given that Si is somewhat distorted from the C_{60} surface geometrically, if it is surrounded by molecules, a bond between the molecule and fullerene will be created from the Si dopant.

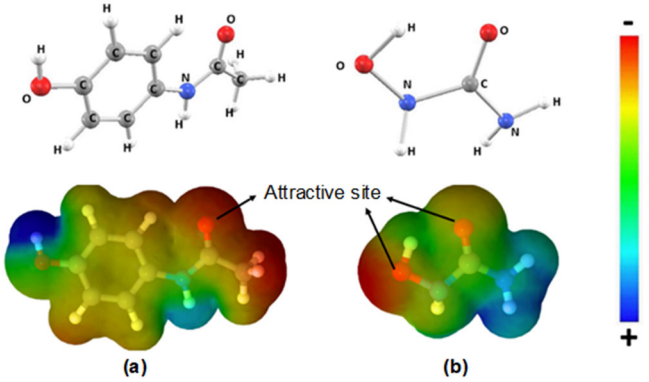

Fig 1. Optimized geometry and MEP plot of (a) paracetamol and (b) hydroxyurea. Less to more attractive sites are shown from blue to red

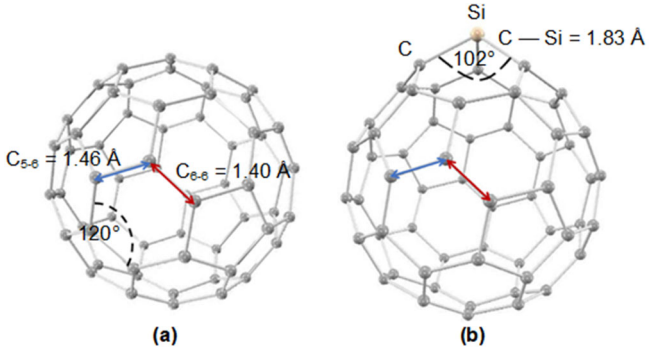

Fig 2. Optimized geometries of (a) pure C_{60} and (b) Si-doped fullerene (SiC_{59})

The optimized geometries of the C_{60} and SiC_{59} with paracetamol and hydroxyurea drug molecules are shown in Fig. 3. Pristine fullerene and drug molecules do not create a bond, whereas the Si-doped fullerene creates a bond between Si and the attractive site oxygen atom from the drug molecules. The drug interaction with Si-doped fullerene resulting in a C–Si–C angle in the hexagonal site is about 108° which increases ~6° from Si-doped fullerene without drug molecules. The Si–O bond (Fig. 3) aligns with the findings that the vicinity of the oxygen atom provides a suitable region for drug molecules to interact with other molecules, exhibiting an attractive characteristic (Fig. 1), and the distorted Si atom from the fullerene (Fig. 2). Additionally, in the pristine fullerene the distance C–O, C–N, C–C are similar in the paracetamol (Fig. 3(a)) and hydroxyurea (Fig. 3(c)), meanwhile in the Si-doped fullerene only atom in the attractive site (oxygen atom) produces a bond

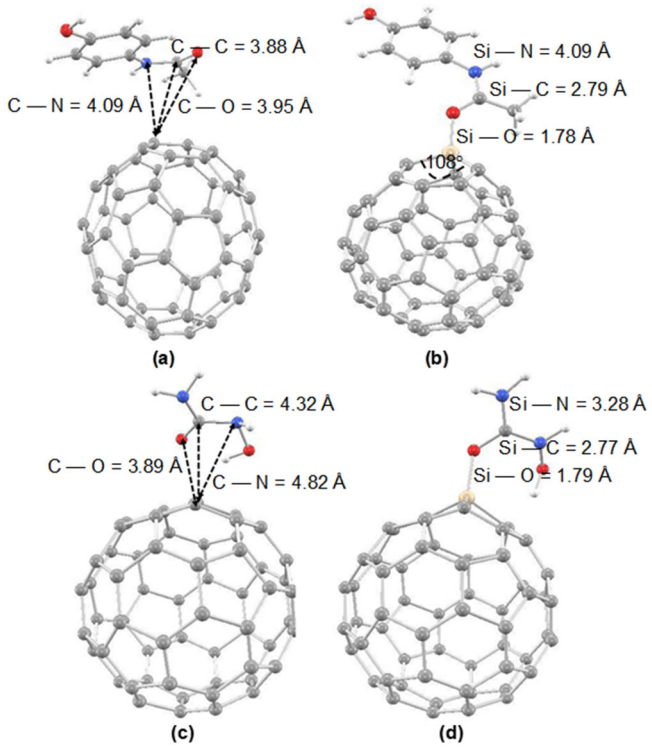

Fig 3. Optimized geometries of (a) pure C_{60} with paracetamol and (b) Si-doped fullerene (SiC_{59}) with paracetamol (c) pure C_{60} with hydroxyurea and (d) Si-doped Fullerene (SiC_{59}) with hydroxyurea

with the Si atom from the fullerene (Figs. 3(b) and 3(d)). The active interaction between the attractive site from drug molecules and the Si-doped fullerene results in a shortened distance between drug molecules and the fullerene. The distance between oxygen and Si atoms in the SiC_{59}–Para and SiC_{59}–HU systems decrease almost twice that between oxygen and carbon atoms in the C_{60}–Para and C_{60}–HU systems.

Energy Calculation

The calculated energies of the system are given in Table 1, which shows that the addition of the Si dopant decreases the energy gap between C_{60}–drug and SiC_{59}–drug. The energy gap of the SiC_{59} system is 0.93 eV, which is lower than that of C_{60}. The energy gaps of SiC_{59}–Para and SiC_{59}–HU have decreased by 0.14 and 0.49 eV, respectively, relative to those of C_{60}–Para and C_{60}–HU. A reduction in the energy gap results in low binding energy needed in the interaction [34,37].

Next, the formation energy was calculated. The formation energy is the energy needed to change one doped atom in the system. A low formation energy indicates that the system is stable. Table 1 shows that the formation energy of SiC_{59}–Para and SiC_{59}–HU is ~0.69 eV lower than that of SiC_{59}.

A positive adsorption energy indicates that the interaction between molecules is physisorption without charge transfer; meanwhile, a negative adsorption energy indicates that the interaction between molecules is exothermic, geometrically stable, and involves charge [23]. Negative adsorption energy also shows that the adsorption between molecules is chemisorption. All systems with drug molecules in Table 1 have negative adsorption energies. The system of Si-doped fullerene with drug molecules has high adsorption, e.g., the adsorption of SiC_{59}–Para and SiC_{59}–HU is 50 times higher than that of the C_{60}–Para and C_{60}–HU systems. The reduction in the bandgap of the SiC_{59}–drug by the Si dopant increases the adsorption between drug molecules and fullerene. Geometrically, the high adsorption between Si-doped

Table 1. Calculated energies of the systems: energy gap, adsorption energy, and formation energy of the system

System	E_s (eV)	E_{HOMO} (eV)	E_{LUMO} (eV)	E_g (eV)	E_{ads} (eV)	E_f (eV)
Paracetamol	−2521.74	0.13	3.53	3.40	-	-
Hydroxyurea	−1628.63	0.13	4.43	4.30	-	-
C_{60}	−9262.96	0.14	1.50	1.36	-	-
$C_{59}Si$	−9213.78	0.14	1.06	0.93	-	2.55
C_{60}-Para	−11784.73	0.13	0.89	0.76	−0.03	-
$C_{59}Si$-Para	−11736.79	0.15	0.78	0.63	−1.27	1.31
C_{60}-HU	−10891.62	0.13	1.35	1.22	−0.03	-
$C_{59}Si$-HU	−10843.58	0.13	0.87	0.73	−1.16	1.41

Table 2. ECT calculations of the systems

System	μ	η	ω	ΔN_{max}	χ	ECT (e)	Note
Paracetamol	1.83	1.70	0.99	−1.08	−1.83	-	-
Hydroxyurea	2.28	2.15	1.21	−1.06	−2.28	-	-
C_{60}	0.82	0.68	0.50	−1.21	−0.82	-	-
$C_{59}Si$	0.60	0.46	0.39	−1.29	−0.60	-	-
C_{60}-Para	0.51	0.38	0.34	−1.34	−0.51	0.13	drug acceptor
$C_{59}Si$-Para	0.47	0.31	0.35	−1.48	−0.46	0.22	drug acceptor
C_{60}-HU	0.74	0.61	0.45	−1.21	−0.74	0.15	drug acceptor
$C_{59}Si$-HU	0.50	0.37	0.34	−1.36	−0.50	0.23	drug acceptor

fullerene and the drug molecules is illustrated by the creation of a Si–O bond in the optimized geometry (Fig. 3). Initially, the Si atom that replaces C in fullerene is in an sp^2 hybridization state. By interacting with paracetamol and hydroxyurea, Si creates a bond with oxygen, thus entering an sp^3 hybridization state.

The electrophilic index, chemical reactivity, and chemical hardness were then calculated to determine the reactivity and chemical stability of the compounds. Chemical hardness is one important parameter for determining the structures and activities of molecules. Table 2 shows that the chemical hardness of Si-doped fullerene with drug molecules (paracetamol and hydroxyurea) is lower than that of the individual drug molecule. This result indicates that the systems of SiC_{59}–Para and SiC_{59}–HU are more active and have higher adsorption levels than other systems.

The electrophilicity index and maximum charge transfer are also considered to be major parameters for determining the tendency of a molecule to adsorb electrons. Compounds with low electrophilicity can transfer electrons, whereas those with high electrophilicity can accept electrons. Table 2 shows that Si-doped fullerene has a lower electrophilicity index than the drug molecules. Electrophilicity indexes are used to determine the charge transfer (ECT) between drug molecules and fullerene. The ECT value of the Si-doped fullerene with drug molecules is ~0.7 e higher than that of the undoped fullerene system with drug molecules. Therefore, more charges are transferred during the adsorption of a drug onto fullerene.

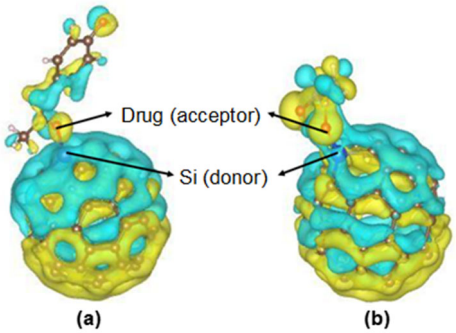

Fig 4. Charge density difference plot of (a) pure C_{60} with paracetamol and (b) Si-doped fullerene (SiC_{59}) with hydroxyurea

The charge density difference plots generated by using Eq. (10) are presented in Fig. 4, where yellow and blue represent the gain and loss of charge after adsorption, respectively. The area around Si from fullerene in both systems is blue, indicating that fullerene has lost charge. Meanwhile, the area around oxygen from both drug molecules is yellow, indicating that the drug molecules have gained charges. Therefore, charges flowed from fullerene to the drug molecules. This result agrees with the positive ECT values obtained through the electrophilicity calculation and indicates that paracetamol and hydroxyurea act as acceptors.

■ CONCLUSION

Systems of fullerene and Si-doped fullerene with paracetamol and hydroxyurea were investigated by using DFT calculations. SiC_{59} has a higher adsorption capacity for paracetamol and hydroxyurea than undoped C_{60}. Paracetamol and hydroxyurea behave as acceptors as

indicated by their positive ECT values. As inferred from the energy and ECT calculations, SiC_{59} is a plausible candidate drug delivery system for paracetamol and hydroxyurea.

■ ACKNOWLEDGMENTS

The author would like to thank the Directorate Research Universitas Gadjah Mada for the RTA-2022 (*Rekognisi Tugas Akhir*) grant No. 3550/UN1.P.III/Dit-Lit/PT.01.05/2022. The computations were performed using computer facilities at the Department of Physics, Universitas Gadjah Mada, and the ALELEON Supercomputer at EFISON *Lisan Teknologi* HQ, Indonesia.

■ AUTHOR CONTRIBUTIONS

Yosephine Novita Apriati wrote the original paper, visualization, and formal analysis, Bambang Kristiawan contributed to the software and formal analysis, Nikmatul Jannah contributed to the software and method, Ari Dwi Nugraheni did the supervision and formal analysis, Sholihun contributed in supervision, method, formal analysis, and writing original paper.

■ REFERENCES

[1] Housman, G., Byler, S., Heerboth, S., Lapinska, K., Longacre, M., Snyder, N., and Sarkar, S., 2014, Drug resistance in cancer: An overview, *Cancers*, 6 (3), 1769–1792.

[2] Duan, Y., Shen, C., Zhang, Y., and Luo, Y., 2022, Advanced diagnostic and therapeutic strategies in nanotechnology for lung cancer, *Front. Oncol.*, 12, 1031000.

[3] Kazemzadeh, H., and Mozafari, M., 2019, Fullerene-based delivery systems, *Drug Discov. Today*, 24 (3), 298–905.

[4] Sergio, M., Behzadi, H., Otto, A., and van der Spoel, D., 2013, Fullerenes toxicity and electronic properties, *Environ. Chem. Lett.*, 11 (2), 105–118.

[5] Couvreur, P., 2013, Nanoparticles in drug delivery: Past, present and future, *Adv. Drug Delivery Rev.*, 65 (1), 21–23.

[6] Goodarzi, S., Da Ros, T., Conde, J., Sefat, F., and Mozafari, M., 2017, Fullerene: Biomedical-engineers get to revisit an old friend, *Mater. Today*, 20 (8), 460–480.

[7] Kroto, H.W., Heath, J.R., O'Brien, S.C., Curl, R.F., and Smalley, R.E., 1985, C_{60}: Buckminsterfullerene, *Nature,* 318, 162–163.

[8] Felker, P.M., and Bačić, Z., 2020, Flexible water molecule in C_{60}: Intramolecular vibrational frequencies and translation-rotation eigenstates from fully coupled nine-dimensional quantum calculations with small basis sets, *J. Chem. Phys.*, 152 (1), 014108.

[9] Mędrek, M., Pluciński, F.A., and Mazurek, A.P., 2013, Endohedral complexes of fullerene C_{60} with small covalent molecules (H_2O, NH_3, H_2, $2H_2$, $3H_2$, $4H_2$, O_2, O_3) in the context of potential drug transporter system, *Acta Pol. Pharm.*, 70 (4), 659–665.

[10] Bashiri, S., Vesally, E., Bekhradnia, A., Hosseinian, A., and Edjlali, L., 2017, Utility of extrinsic [60] fullerenes as work function type sensors for amphetamine drug detection: DFT studies, *Vacuum*, 136, 156–162.

[11] Moradi, M., Nouraliei, M., and Moradi, R., 2017, Theoretical study on the phenylpropanolamine drug interaction with the pristine, Si and Al doped [60] fullerenes, *Phys. E*, 87, 186–191.

[12] Parlak, C., and Alver, O., 2017, A density functional theory investigation on amantadine drug interaction with pristine and B, Al, Si, Ga, Ge doped C_{60} fullerenes, *Chem. Phys. Lett.*, 678, 85–90.

[13] Hazrati, M.K., and Hadipour, N.L., 2016, Adsorption behavior of 5-fluorouracil on pristine, B-, Si-, and Al-doped C60 fullerenes: A first-principles study, *Phys. Lett. A*, 380 (7-8), 937–941.

[14] Apriati, Y.N., Nugraheni, A.D., and Sholihun, S., 2022, Interaction of C_{60} with small molecules: Adsorption - inclusion energy calculation using the density functional theory, *Mater. Sci. Forum*, 1066, 135–143.

[15] Gökpek, Y., Bilge, M., Bilge, D., Alver, Ö., and Parlak, C., 2017, Adsorption mechanism, structural and electronic properties: 4-Phenylpyridine &

undoped or doped (B or Si) C60, *J. Mol. Liq.*, 238, 225–228.

[16] Bagheri Novir, S., and Aram, M.R., 2020, Quantum mechanical simulation of chloroquine drug interaction with C_{60} fullerene for treatment of COVID-19, *Chem. Phys. Lett.*, 757, 137869.

[17] Bibi, S., Urrehman, S., Khalid, L., Yaseen, M., Khan, A.Q., and Jia, R., 2021, Metal doped fullerene complexes as promising drug delivery materials against COVID-19, *Chem. Pap.*, 75 (12), 6487–6497.

[18] Sholihun, S., Saito, M., Ohno, T., and Yamasaki, T., 2015, Density-functional-theory-based calculations of formation energy and concentration of the silicon monovacancy, *Jpn. J. Appl. Phys.*, 54, 041301.

[19] Umam, K., Sholihun, S., Nurwantoro, P., Ulil Absor, M.A., Nugraheni, A.D., and Budhi, R.H.S, 2018, Biaxial strain effects on the electronic properties of silicene: The density-functional-theory-based calculations, *J. Phys.: Conf. Ser.*, 1011, 012074.

[20] Sholihun, S., Khadarisman, H.P., and Nurwantoro, P., 2018, Density-functional-theory calculations of formation energy of the nitrogen-doped diamond, *Indones. J. Chem.,* 18 (4), 749–754

[21] Yamasaki, T., Kuroda, A., Kato, T., Nara, J., Koga, J., Uda, T., Minami, K., and Ohno, T., 2019, Multi-axis decomposition of density functional program for strong scaling up to 82,944 nodes on the K computer: Compactly folded 3D-FFT communicators in the 6D torus network, *Comput. Phys. Commun.*, 244, 264–276.

[22] Perdew, J.P., Burke, K., and Ernzerhof, M., 1996, Generalized gradient approximation made simple, *Phys. Rev. Lett.*, 77, 3865.

[23] Vuong, B.X., Hajali, N., Asadi, A., Baqer, A.A., Hachim, S.K., and Canli, G., 2022, Drug delivery assessment of an iron-doped fullerene cage towards thiotepa anticancer drug, *Inorg. Chem. Commun.*, 141, 109558.

[24] Bongu, R.S., Bisht, P.B., Namboodiri, R.C.K., Nayak, P., Ramaprabhu, S., Kelly, T.J., Fallon, C., and Costello, J.T., 2014, Influence of localized surface plasmons on Pauli blocking and optical limiting in graphene under femtosecond pumping, *J. Appl. Phys.*, 116 (2), 073101.

[25] Yang, Y., Arias, F., Echegoyen, L., Chibante, L.P.F., Flanagan, S., Robertson, A., and Wilson, L.J., 1995, Reversible fullerene electrochemistry: Correlation with the HOMO-LUMO energy difference for C_{60}, C_{70}, C_{76}, C_{78}, and C_{84}, *J. Am. Chem. Soc.*, 117 (29), 7801–7804.

[26] Ren, S.L., Wang, Y., Rao, A., McRae, E., Holden, J.M., Hager, T., Wang, K.A., Lee, W.T., Ni, H.F., Selegue, J., and Eklund, P.C., 1991, Ellipsometric determination of the optical constants of C_{60} (Buckminsterfullerene) films, *Appl. Phys. Lett.*, 59 (21), 2678–2680.

[27] Parr, R.G., Szentpály, L.V., and Liu, S., 1999, Electrophilicity index, *J. Am. Chem. Soc.*, 121 (9), 1922–1924.

[28] Maynard, A.T., Huang, M., Rice, W.G., and Covell, D.G., 1998, Reactivity of the HIV-1 nucleocapsid protein p7 zinc finger domains from the perspective of density-functional theory, *Proc. Natl. Acad. Sci. U. S. A.*, 95 (20), 11578–11583.

[29] Padmanabhan, J., Parthasarathi, R., Subramanian, V., and Chattaraj, P.K., 2007, Electrophilicity based charge transfer descriptor, *J. Phys. Chem. A*, 111 (7), 1358–1361.

[30] Momma, K., and Izumi, F., 2011, VESTA 3 for three-dimensional visualization of crystal, volumetric and morphology data, *J. Appl. Crystallogr.*, 44, 1272–1276.

[31] Al Fauzan, M.F., Satya, T.P., Setyawan, G., Fahrurrozi, I., Puspasari, F., Partini, J., and Sholihun, S., 2021, Adsorption of toxic heavy metal methylmercury (MeHg) on germanene in aqueous environment: A first-principles study, *Indones. J. Chem.*, 21 (6), 1484–1490.

[32] Al-Fauzan, M.R., Astuti, W.D., Al-Fauzan, G., and Sholihun, S., 2018, A first-principles investigation of the adsorption of CO and NO molecules on germanene, *IOP Conf. Ser.: Mater. Sci. Eng.*, 367, 012051.

[33] Jmol Development Team, 2016, *Jmol: An open-source Java viewer for chemical structures in 3D*, http://jmol.org/.

[34] Vatanparast, M., and Shariatinia, Z., 2019, Hexagonal

boron nitride nanosheet as novel drug delivery system for anticancer drugs: Insights from DFT calculations and molecular dynamics simulations, *J. Mol. Graphics Modell.*, 89, 50–59.

[35] Xu, H., Tu, X., Fan, G., Wang, Q., Wang, X., and Chu, X., 2020, Adsorption properties study of boron nitride fullerene for the application as smart drug delivery agent of anti-cancer drug hydroxyurea by density functional theory, *J. Mol. Liq.*, 318, 114315.

[36] Li, M., Wei, Y., Zhang, G., Wang, F., Li, M., and Soleymanabadi, H., 2020, A DFT study on the detection of isoniazid drug by pristine, Si and Al doped C_{70} fullerenes, *Phys. E*, 118, 113878.

[37] Rahman, H., Hossain, M.R., and Ferdous, T., 2020, The recent advancement of low-dimensional nanostructured materials for drug delivery and drug sensing application: A brief review, *J. Mol. Liq.,* 320, 114427.